

The SIM Astrometric Grid

Raymond Swartz

Jet Propulsion Laboratory, California Institute of Technology

ABSTRACT

The Space Interferometry Mission (SIM) is fundamentally a one-dimensional instrument with a 15-degree field-of-regard. Mission objectives require a global reference grid of thousands of well-understood stars with positions known to 4 microarcseconds which will be used to establish the instrument baseline vector during scientific observations. This accuracy will be achieved by frequently observing a set of stars throughout the mission and performing a global fit of the observations to determine position, proper motion and parallax for each star. Each star will be observed approximately 200 times with about 6.5 stars per single instrument field on the sky. We describe the nature of the reference grid, the candidate objects, and the results of simulations demonstrating grid performance, including estimates of the grid robustness when including effects such as instrument drift and possible contamination of the grid star sample by undetected binaries.

Keywords: Space Interferometry Mission, SIM, SIM grid, interferometry, astrometry.

1. INTRODUCTION

When the Space Interferometry Mission (SIM) launches in 2009 it will be the most precise optical astrometric instrument built to date.¹ Positioned in an earth-trailing solar orbit, SIM will be able to do astrometric measurements to a precision never previously achieved. The measurements taken by SIM during its five-year science mission are expected to lead to discoveries of many new extra-solar planets as well as more precisely map out the orbital parameters of known planetary systems, in addition to contributing to a host of non-planetary-system science.

SIM is a 10-meter Michaelson interferometer with a field-of-regard 15 degrees in diameter. In order to monitor the state of the instrument baseline during the mission and to support the wide-angle astrometric goals of the SIM mission with the one-dimensional narrow angle instrument, we will maintain a 4π astrometric model of a set of stars to serve as an external astrometric calibration for the instrument baseline.

1.1. Interferometer Basics

The basic operation of an interferometer involves precise measurement of the internal delay-line required to cause light following two different paths inside the instrument to constructively interfere with itself, as shown in Figure 1. The only direct observable from the instrument is the internal delay-line-setting required to achieve constructive interference for the light. By the nature of the instrument this measurement is one-dimensional.

The governing astrometric equation for interferometric measurements for an interferometer is

$$d = \vec{s} \cdot \vec{B} + C() = l(\vec{s} \cdot \vec{b}) + C() \quad (1)$$

where d is the optical delay (units of length) measured by the interferometer, \vec{s} is the unit position vector for the star we are observing and $\vec{B} = l\vec{b}$ is the interferometer baseline vector which can be broken up into its length (l) and orientation (\vec{b}) components. We see by separating the baseline length and orientation terms that the baseline length sets the scale of the impact of the angular measurements. The function $C()$ represents a bias function for a real-world non-ideal instrument, which may depend on time, instrument orientation, and stellar position in the field of regard. For discussion purposes we shall assume an ideal instrument and assume $C() = 0$.

The laser metrology system on SIM² precisely tracks and compensates for changes in the instrument baseline length. At the start of the mission, the length of the baseline is not known precisely enough to achieve the ultimate mission objectives. We use the ability of the metrology system to track and compensate for length changes to give us the stability we need for the long-term observations of the grid stars to establish the baseline length for the mission science observations. This determination is critical since, as seen in Equation 1 we need detailed knowledge of the baseline length is needed to set a scale for the observations. We achieve this goal by a bootstrap method of taking a series of measurements of the grid stars during the mission and performing a global fit of the data, allowing the 4π nature of the celestial sphere to constrain the global scale of the problem.

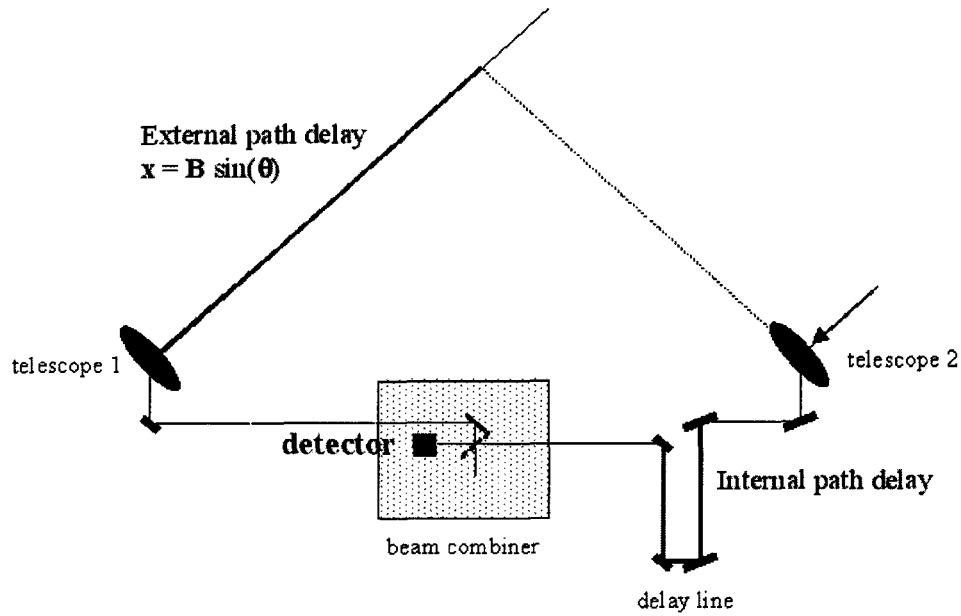


Figure 1. The basic components of an interferometer. The peak detection intensity occurs when the external delay and the internal delay lines are equal, which gives a precise measurement of the angle between the baseline orientation and the light source.

2. THE SIM GRID

While doing the science observations of the SIM mission, for each instrument field-of-regard we shall also make repeated observations of a set of well-understood astrometrically simple stars scattered around the celestial sphere. These observations will provide important instrument calibration parameters as we will then perform global fit of the observations to find the stellar parameters for these stars as well as the instrument baseline vectors during the observations. The 4π nature of the celestial sphere then locks in the stellar positions and sets the length scale for the instrument.

The SIM Grid is to serve as a series of “surveyor’s landmarks” on the celestial sphere to allow determination of the baseline vector during science observations. The astrometric parameters of the grid stars will be determined by a global optimization process. In order to accurately model and understand the stellar motion, we need well-understood astrometrically simple stars, so we want to avoid stars with any characteristic that complicates its motion, including starspots and substantial orbiting companions. Even variations in stellar magnitude may affect the way the light propagates through the SIM instrument or perhaps be an indicator of an eclipsing multiple star system, so we will also avoid stars with detectable variability.

Avoiding multiple star systems is a special problem in that, prior to launch, ground observations will be all that we have available to filter out stars with companions. Since the precision of SIM measurements will be much higher than ground-based observations, we fully expect that there will be some problem stars that will make it through the filtering process, and expect to have to carry sufficient “extra” stars in the grid catalog to compensate for expected contamination.

2.1. The Grid Population

There are two opposing requirements on the selection of stable grid star candidates. We want stars bright enough to be observed quickly so as not to cut into available mission time for science observations, yet we want stars with a small angular size so they are not resolved as other than a point source by the instrument. We are also compelled to prefer farther stars by wanting to minimize the angular stellar reflex motion caused by any possible orbiting companions is reduced.

A plentiful population of such stars are found in metal-poor K giants. The metal-poor nature of these stars makes them bright, even when placed at large distances of a kiloparsec or more. Our understanding of these stars also leads us to believe that there will be no problems with starspots or other peculiarities.

3. GRID OBSERVATIONS

We define a *tile* as a set of observations tied to a single baseline configuration. Observing the stars of interest in the field of regard while keeping the baseline steady will tie those observations together and allow determination of the baseline parameters. Note that leaving a particular area of the sky and then returning to it establishes a new tile; we have no expectation that the same baseline orientation will be reestablished. Once a tile is completed, the spacecraft is reoriented so that the field-of-regard covers a new region of the sky and the observations continue.

Holding the baseline steady while we measure each star in the tile ties those observations together to a consistent baseline vector, but we also need to tie adjacent tiles together in order to create a the full 4π grid. We use an overlap region between the tiles to accomplish this. By observing a series of tiles with tile-to-tile overlaps in the observed region, as shown in Figure 2, we tie the tiles together to obtain wide-angle results from our narrow-angle instrument.

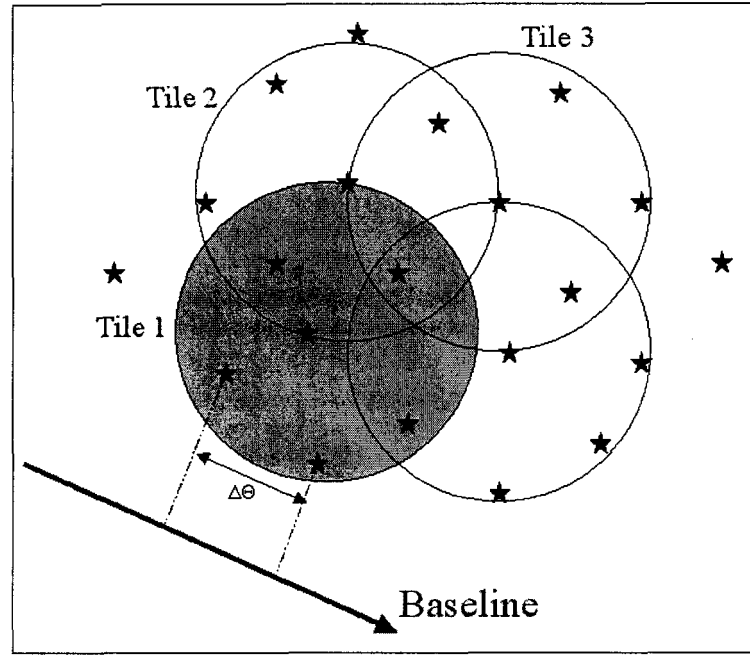


Figure 2. The tiles are observed on the sky in a step-wise fashion. Maintaining the baseline orientation for all of the stars in the tile will tie those observations together, while the stars in the tile overlap region will tie adjacent tiles together. This process is repeated for the entire sky. This diagram also shows that the only way to tie together widely separated stars is through the tile-to-tile overlap, demonstrating the importance of the overlap region.

Observations are currently ongoing³ to find candidate grid objects by observing the sky in 1302 regions of the sky we call *bricks*, approximately 1.0×0.3 degrees laid out in a semi-regular pattern on the sky, as seen in Figure 3. This strategy permits detailed study of candidate objects while allowing even distribution of the grid stars.

3.1. Orange Peel Scan Model

The working model we've used to date for the grid observation sequence during the 5-year SIM mission is a series of 23 full-sky scans minus the solar exclusion region. Each scan starts with a tile centered on the brick nearest the anti-sun direction. We then center a tile on each adjacent brick, slowly spiraling toward the sun until we reach the outer edge of the solar exclusion region, which for the purposes of our simulations has been set to 45 degrees. This part of the scan requires about one thousand tiles.

Once we have covered the edge of the solar exclusion region, we then center a tile on each brick spiraling back out to the anti-sun direction, this time with the baseline orthogonal to the direction in had when that region of the sky was

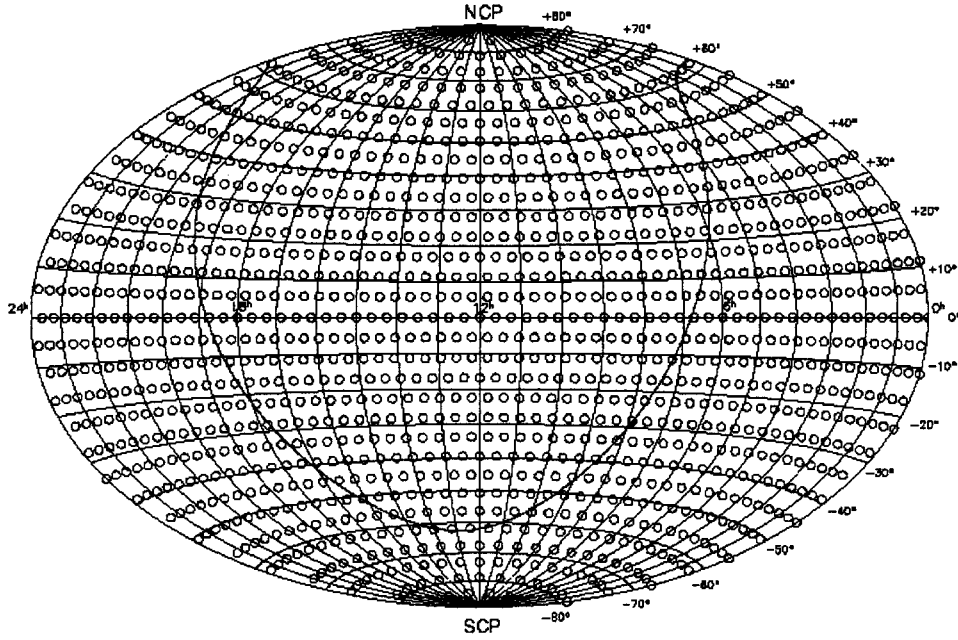


Figure 3. Locations of the Bricks described in the text. The line through the diagram is the galactic plane.

last observed.. We do this to compensate for the fundamental one-dimensional nature of the instrument so that we have isotropic measurement uncertainties. On this second pass, there is no requirement that the tile centers be exactly the same as they were for the first pass, since we are solving for an independent set of baseline parameters on the second pass.

This process is repeated every several months during the orbit of SIM around the sun. The new location of SIM in its orbit insures that the solar exclusion region from the first set of observations is filled in, and 4π coverage is achieved. A global fit of these observations determines the stellar parameters and the instrument baselines. Our current working model involves repeating this process approximately 4.5 times a year. Again, there is no requirement that the next time we cover the sky the baseline orientations or the tile centers be the same as the previous visit to a region of the sky.

3.2. Simulating The Grid

We use a simulation of the SIM instrument and grid observation sequence to determine characteristics of the grid measurements and the effects of instrument design decisions. The simulation is also useful in developing solution techniques for the large amount of observation data expected. This simulation includes generating a set of grid stars, determining our pre-mission knowledge of these objects, and the observation sequence that will be used to perform the measurements. This simulation process provides a set of simulated measurements for data reduction software development.

3.2.1. Generating The Catalogs

Using the brick locations discussed earlier as a working starting point, we create a catalog of “true” stellar positions by randomly generating a single grid star in each brick. Proper motion for these stars is generated using a gaussian distribution with $\sigma = 1 \mu\text{as}$ in a random direction. Each star is placed at a randomly generated gaussian distance of 1.0 ± 0.1 kiloparsecs in order to simulate the parallax effects in the measurements.

To generate the a priori catalog representing our knowledge of the objects at mission start, we take the parameters from the generated truth catalog and apply a gaussian perturbation to the stellar parameters. The perturbation sigmas we currently use are 0.1 arc-second(as) for the position, 2 mas/yr for the proper motion, and 2 mas for the parallax. The values from this perturbed a priori catalog are used for the initial estimate of the stellar positions during the fitting process.

3.2.2. Generating The Simulated Measurements

There are two steps to generating the simulated observations. First, we create an observation sequence detailing the instrument pointing vectors at specific epochs. The current observation model we used has been called the “orange peel” approach, in which we start each whole-sky scan by pointing in the anti-sun direction and stepping tile by tile in a spiral toward the sun, where each tile is centered on the nearest brick. Once we reach the closest angle to the sun we can observe (approximately 50 degrees in the current design) we spiral back out toward the anti-sun direction. During this second pass we use a baseline orientation that is orthogonal to the previous baseline orientation for each field-of-regard. This process is timed to take place approximately 4.5 times per year, and in total gives us our baseline orientations and boresight pointings for the entire mission.

To generate the simulated measurements we step through the list of baselines. For each baseline we determine from the perturbed catalog which stars are expected to be in the field-of-regard at the measurement epoch and, for those stars, we then use the true catalog position (propagated to the observation epoch) for the grid star, and use Equation 1 with an added gaussian measurement error to generate a delay measurement for that observation. Simulating a five-year mission involves generating over 300,000 such observations over 46,000 tiles.

4. PROCESSING THE GRID OBSERVATIONS

We characterize the grid stars with a basic set of five astrometric parameters: position, proper motion and parallax. A global fit of the data to determines the stellar parameters as well as the interferometer baseline orientations and lengths during the observation tiles. Every tile has a different unique baseline orientation, but we can treat the baseline lengths a bit differently for added leverage (in the observations per parameter sense). We expect some variation in the baseline length, but it is also reasonable to assume that there be some continuity in the length from tile to tile. In other words, while the baseline will change the rate will be slow enough that solving for a single baseline length value for a number of chronologically adjacent tiles is a valid approach.

The fitting process uses as input a catalog of the a priori information for the grid stars and the measurement set, which is a list of the objects observed, the observation epochs, and the measured delays. As a first step, in the measurement process, the a priori star catalog is used with the relevant observations to determine an initial estimate of the instrument baseline parameters.

These a priori baseline and stellar parameters are then used to establish a model of the SIM observations via Equation 1 to calculate a set of “model delays”. In the real world, the measurements made by the instrument are not ideal, and the uncertainties inherent in reality require us to find a best fit using an optimization method, to minimize

$$\min_{\mathbf{x}} \|\mathbf{A}\vec{\mathbf{x}} - \vec{\mathbf{b}}\|. \quad (2)$$

The matrix \mathbf{A} is known as the design matrix, $\vec{\mathbf{x}}$ is a vector of the corrections parameters we are trying to determine, and $\vec{\mathbf{b}}$ is a column vector of the delay *differences* between the actual measured delay and the measurement predictions based on the current values of our stellar and instrument model parameters:

$$b_i = d_i - (\vec{\mathbf{s}}_i \cdot \vec{\mathbf{B}} + C)_{model} \quad (3)$$

The design matrix \mathbf{A} consists of the partial derivatives with respect to the astrometric and instrumental parameters. The form of \mathbf{A} is derived from Equation 1 and details in how the model parameters (baseline, proper motion, etc.) enter into the values for $\vec{\mathbf{s}}$, $\vec{\mathbf{B}}$ and C . By construction the only non-zero elements of each row of \mathbf{A} contains the model parameters of one observation at a particular epoch, leading to a large but sparse design matrix.

The large size and sparseness of \mathbf{A} makes the direct solution of Equation 2 via

$$\mathbf{x} = (\mathbf{A}^T \mathbf{A})^{-1} \mathbf{A}^T \vec{\mathbf{b}} \quad (4)$$

unwieldy because of the calculation of the inverse. However, because of the sparseness of \mathbf{A} , we have an approach available in the associated linear system of normal equations

$$(\mathbf{A}^T \mathbf{A})\mathbf{x} = (\mathbf{A}^T \vec{\mathbf{b}}). \quad (5)$$

A convenient iterative solution method for this system is available in the Conjugate Gradient on the Normal Equations.⁴ In short, this method successively propagates “down the slope” along the steepest gradient until a minimum is reached. Using this method, we solve for the vector of corrections to the model parameters, apply the corrections to the model, recalculate the difference vector $\vec{\mathbf{b}}$. This iterative process is repeated until the norm of the correction vector is less than some predetermined value, in which we can say that the solution has converged.

4.1. Pin Objects

We still have a problem with the setup of this problem because the matrix is under determined, in that there is a null space. In other words, the stellar coordinates and the instrument baselines can both rotate freely as the problem is stated. We need something on which to anchor the solution, so we define *pin objects* as two selected grid objects for which we will not fit all the parameters. Instead we will assume the 5-parameter a priori information for one of these objects is accurate. This fixes one point on the celestial sphere, but we still have a problem with the sphere rotating around that object. We then assume the a priori information for the azimuthal angle of the second pin object around the first pin object is also accurate to pin down the rotation of the sphere. By nailing down these two points on the sphere, we have then eliminated the null-space and allowed a frame for the solution.

Note that while the pin objects eliminate the null space in the matrix, they do not completely eliminate the problem of a global rotation of the frame. There is still some residual rotation because of measurement errors while the pin objects are being observed. So, after the matrix is solved, we apply a global rotation to the fitted grid catalog to best align it with

During the mission, we expect to use a set of quasars to tie the optical coordinate frame determined by the grid to the already known VLBI radio reference frame.⁵

The following table shows the number and types of fit parameters for a typical case where we fit for stellar parameters, baseline orientation, instrument bias, and baseline lengths. Note that having more stellar observations per baseline length value means we can better determine the length, however, if the length is changing in reality (as we expect it to) this model will have problems. This is discussed below.

Parameter	n	Total
Stellar Parameters (5 per star)	1,300	6,500
Baseline Orientation (2 per tile)	48,000	96,000
Instrument Bias (1 per tile)	48,000	48,000
Baseline Length (1 per 1000 tiles)	48	48
Total		150,548

Table 1. Breakdown of the parameters used in a sample grid fit.

5. GRID PERFORMANCE RESULTS

Analyzing the grid performance in the simulation is straightforward. We compare the stellar parameters from the generated truth catalog with those of the catalog resulting from the fitting process. Generally, for a single measurement accuracy of $10 \mu\text{as}$ (485 pm random gaussian metrology error) we see a results shown in Table 2.

These results are shown in a bit of detail in Figure 4. We note in the histograms in the first column that the position residuals have a well-behaved gaussian distribution. In the other columns we consider the behavior of the residual across the sky and note that there are no surprising trends. Note that in the last column the “banding” is caused by the distribution of the bricks in Declination, as seen in Figure 3.

Parameter	Value
Mission Lifetime	5 yrs
Total number of whole-sky grid observations	23
Solar Exclusion Angle	45 deg
Single Measurement accuracy	485 pm (10 μ as)
Stellar Position	$2.1 \pm 0.2 \mu$ as
Stellar Proper Motion	$2.0 \pm 0.5 \mu$ as
Stellar Parallax	$2.2 \pm 0.2 \mu$ as

Table 2. The mean value of the sigma of the residuals of the grid fitting process for seven simulation runs. The standard deviation of the results is also shown.

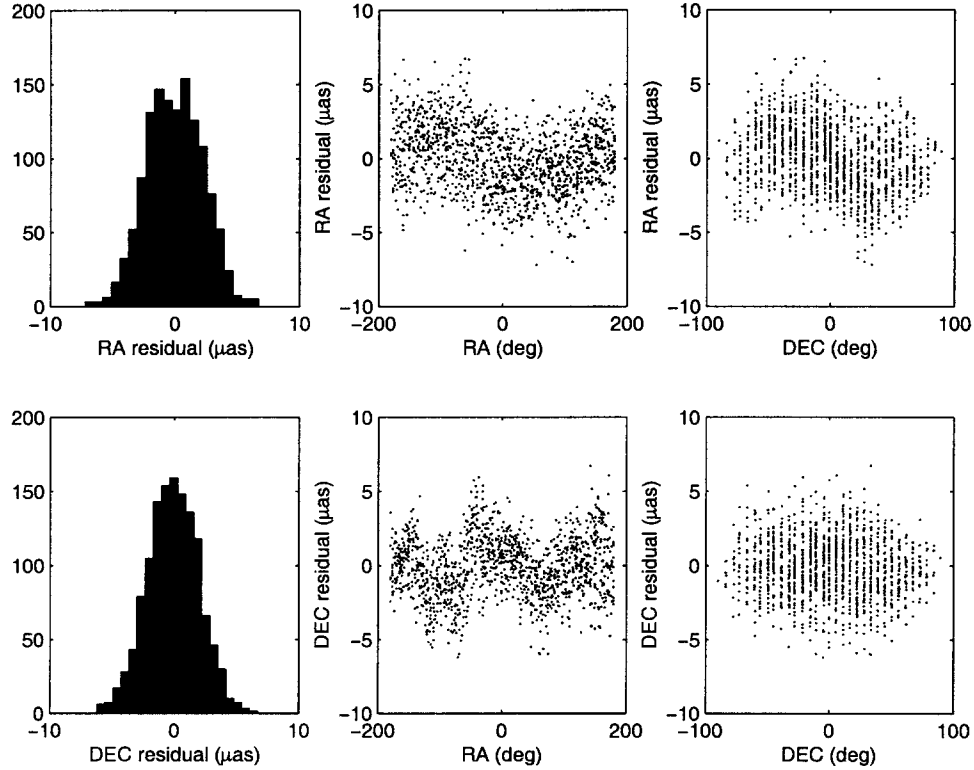


Figure 4. Sample results of the grid fitting procedure, showing only the position residuals and the behavior of those residuals across the sky, as described in the text.

5.1. Zonal Errors

We note that the bottom-middle plot in Figure 4 shows two types of residual error in the estimated parameters of the stars. we see a statistical “scatter” error with a full width of about 5μ as superimposed on a much more systematic “zonal” error, or a slow variation of the mean of the residual as we move around the sky in right ascension. This effect is much more pronounced in a different plot made from the same simulation, seen in Figure 5. These two types of errors will affect different types of science in different ways. For example, a wide angle science result that ties results from two widely separated tiles will have to use both error terms, while a result dealing only with a local region may use the local statistical error only. The details of these decisions depend on the type of science being done. Studies investigating this zonal error in more detail are ongoing.

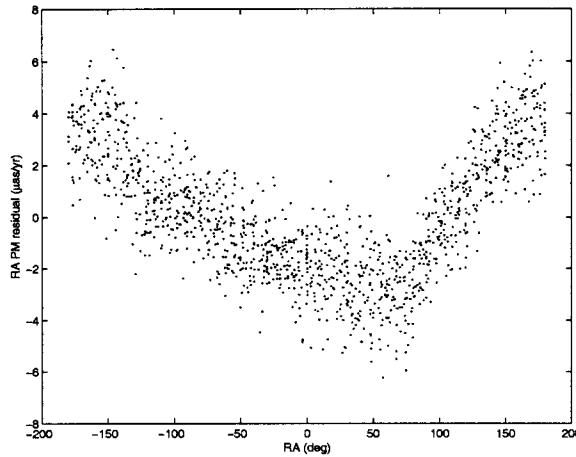


Figure 5. Declination proper motion residuals plotted against right ascension. of the grid fitting procedure. Note that the local and global errors are different, representing statistical and systematic components. This phenomena of zonal errors means it may be possible to use different error scales for local and global science studies.

5.2. Instrument Baselines

The main purpose for the astrometric grid is to determine the baselines during the science observations. If each

6. GRID STABILITY WITH BASELINE DRIFTS

As a test of grid stability and to simulate a real-world condition, we decided to see what happened to the grid if the interferometer baseline was not constant. We modeled this by having the baseline length drift over the course of the mission as in a random walk, and to see what the effect on the grid was, and what can be done to compensate for this effect in the solution process.

We do not expect the baseline length to be constant. In fact, with changing solar angles and such, we expect the baseline to change constantly. The metrology system will track these changes, but there will still be some drift that falls below the precision of the metrology system. A canonical number we have been using for this untracked baseline drift is 800 pm per 5 hours; so that every 5 hours the metrology will change by a gaussian random-walk distance of 800 pm.

When we started these studies, we initially thought that the grid would have to be observed in dedicated “grid stars only” campaigns. The idea was to get a “snapshot” of the instrument and celestial situation in as short of time as possible so that drifts would not be a problem. We expected instrument drifts to cause such problems that an adequate solution would be unachievable. Using this observation scenario the grid would get a dedicated 20% of the mission times, divided into 23 campaigns of about 2.2 weeks each in order to determine the grid star parameters with minimal instrument drift interference. This calculation resulted in about 20 minutes per grid tile so we believed baseline length drifts would not have much time to accumulate. This approach is inefficient in that during the science observations we would have to re-observe grid objects to establish the baseline.

We thought a more efficient use of mission time would be to integrate the grid and science observations. In this way, the grid observations would be scattered over 100% of the mission time, with science observations inserted into each tile, so that each tile was about 100 minutes long.

For this study we only apply the drift between tiles. For the 20% case (20 minute tiles) we applied 20 minutes of baseline length drift at the beginning of each tile, and for the 100% case we applied an accumulated 100 minutes of drift to the length.

We expect that if we solve for baseline lengths infrequently, the accumulated drift will render the results poorly determined. Also, if we solve for a new baseline length for every tile, we will have a significant number of parameters to solve for, causing problems. Recall that there are approximately 46,000 tiles during the mission, so that would be 46,000

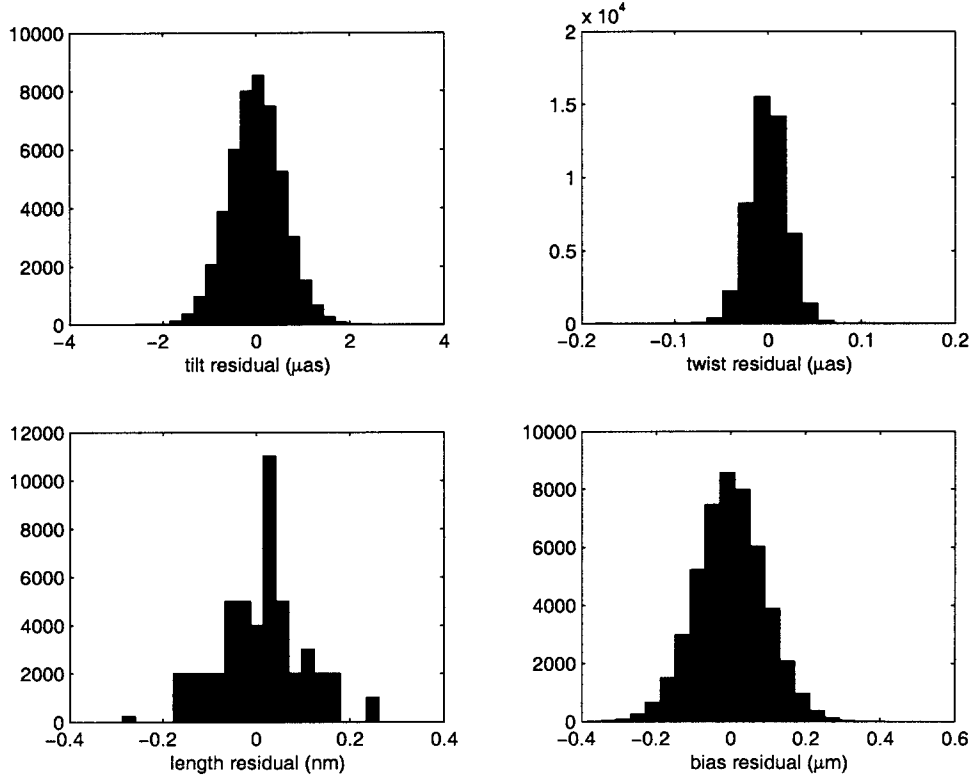


Figure 6. Plot of baselines determined from the grid, and a baseline determined solely from the fitted grid star parameters.

parameters added to the fit, making the fit poorer. In each case, we use as a metric simply the sigma of the stellar position residuals (fitted position minus true position).

In solving the system, we solve for a baseline length value for every tile, then every 3 tiles, then every 5 tiles, and so on, all on the same dataset. In this way, we determine that there is an optimal parameterization for the data to compensate for baseline length drift.

Figure 7 shows the result. We see the expected degradation in grid accuracy for a new baseline fit for every tile (the left side of the plot) and, as we fit for only one baseline length per thousand tiles, at the right end of the plot, we see that performance degrades there as well. We also see the effect of “spreading out” the grid star observations over the mission, in that the 100% case performs much worse than the 20% case. In all cases, though, we see that there is a middle ground, of around 50-100 tiles per baseline length value, where we can minimize the impact of the drifting baseline length.

Thus, we conclude that if the data is handled in the right way we can operate in a the more-efficient mode of combining the grid and science observations in each tile.

7. CONCLUSIONS AND FUTURE STUDIES

We have shown the feasibility of the SIM astrometric grid to determine the spacecraft orientation during the mission. Simulations have shown the grid to be robust under expected conservative models of instrument baseline drifts. While we do see some zonal errors in the solution, we expect to be able to develop techniques based on delay residuals to recognize and quantify these during the mission.

We are currently studying the effectiveness of the SIM grid to verify field-dependent instrument calibrations.

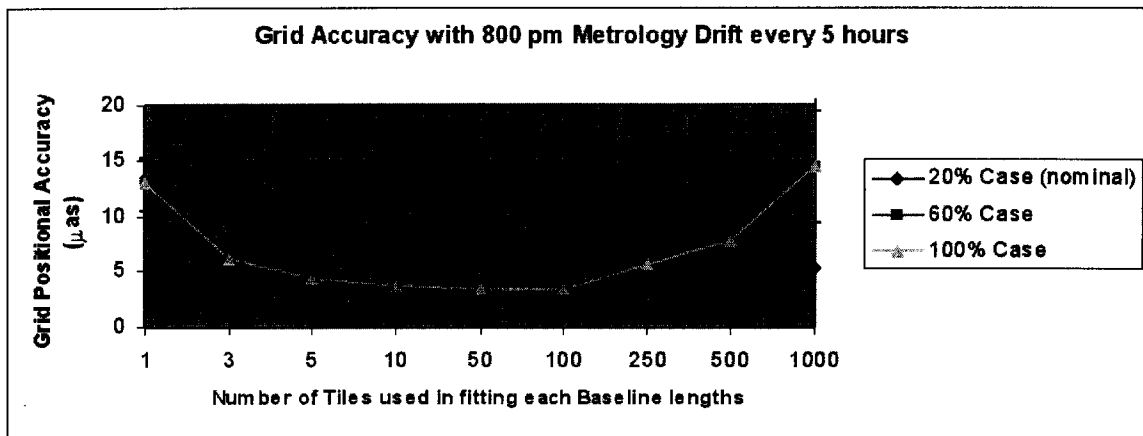


Figure 7. The effect of Baseline Drift. The percentage cases denotes how much of the mission time is used for scattering the grid observations, as described in the text. The 20% case corresponds to 20-minute tiles, while the 100% case has 100-minute tiles. Note that in each case, the most accurate fit for the grid is when a new baseline length is fit about every 50-100 tiles.

8. ACKNOWLEDGMENTS

The research described in this paper was carried out by the Jet Propulsion Laboratory, California Institute of Technology, under a contract with the National Aeronautics and Space Administration.

REFERENCES

1. James C. Marr IV, et al., *Space Interferometry Mission(SIM): Overview and Current Status*, This Volume.
2. Lawrence Ames, et al., *Space Interferometry Mission Starlight And Metrology Subsystems*, This Volume.
3. R Patterson, et al., *The Grid Giant Star Survey for the Space Interferometry Mission*, Small Telescope Astronomy on Global Scales, ASP Conference Series Vol. 246, IAU Colloquium 183, San Francisco: Astronomical Society of the Pacific. p. 65.
4. William H. Press, et al., *Numerical Recipes In C*, p.317, Cambridge University Press, 1988.
5. C. Ma et al., *The International Celestial Reference Frame As Realized By Very Long Baseline Interferometry*, The Astronomical Journal, 116:516-546, July 1998.